Effect of electron correlations on the electronic and magnetic structure of Ti-doped α-hematite

Amrit Bandyopadhyay
Center for Materials for Information Technology and Department of Electrical and Computer Engineering, University of Alabama, Tuscaloosa, Alabama 35487-0209, USA

Julian Velev and W. H. Butler
Center for Materials for Information Technology and Department of Physics, University of Alabama, Tuscaloosa, Alabama 35487-0209, USA
and Metals and Ceramics Division, Oak Ridge National Laboratory, Oak Ridge, Tennessee 37831-6114, USA

Sanjoy K. Sarker
Department of Physics and Astronomy, University of Alabama, Tuscaloosa, Alabama 35487-0209, USA

O. Bengone
Department of Physics, Uppsala University, SE-751 21 Uppsala, Sweden
(Received 30 October 2003; revised manuscript received 17 February 2004; published 28 May 2004)

We study the electronic and magnetic structure of α-hematite and α-hematite doped with Ti using density-functional theory. We use both the local spin-density approximation (LSDA) and the local spin-density approximation with Coulomb correlation (LSDA+U) approximations. We find that as the value of the parameter U is increased, α-hematite(Ti) changes from a magnetic half metal with a single relatively delocalized d electron per Ti to an insulator which has the electron localized on a particular Fe site neighboring the Ti impurity. In contrast to Ti-doped α-hematite, LSDA and LSDA+U are in qualitative agreement for the undoped system, although LSDA+U predicts values of the structural parameters, band gap, and magnetic moments on the Fe sites which are closer to experimental estimates. In general, LSDA+U appears to be better suited for this type of material.

DOI: 10.1103/PhysRevB.69.174429 PACS number(s): 75.50.Pp, 75.50.Gg, 75.50.Ee

I. INTRODUCTION

There is much interest in developing magnetic semiconductors. In order for these materials to be practical they should have a Curie temperature exceeding 400 K. Another very useful property would be the possibility of both *n*- and *p*-type dopings. The issue has been approached along two different paths—first, by doping traditional semiconductors such as InAs,[1] GaAs,[2] GaN,[3] and GaP (Ref. 4) with Mn or other transition metals in order to obtain room-temperature magnetic semiconductors; second, by using nontraditional semiconducting materials that are known to be magnetic at room temperature. An example of a material of the second kind is solid solutions of the minerals ilmenite and α-hematite. Solid solutions of ilmenite ($FeTiO_3$) and α-hematite (corundum structure Fe_2O_3) are potentially interesting spintronic materials because compositions of $(FeTiO_3)_{1-x}(Fe_2O_3)_x$ in the range $0.15<x<0.5$ are known to be semiconducting and also magnetic.[5,6]

In a previous paper,[7] we investigated α-hematite and α-hematite with Ti substituted on some of the Fe sites using density-functional theory within the generalized gradient approximation (LSDA-GGA), where LSDA stands for local spin-density approximation. We concluded that this theory provides a good description of the structural properties of α-hematite. In addition, pure α-hematite was also correctly predicted to be an antiferromagnetic insulator; however, the band gap was underestimated and the magnetic moments on the Fe sites were significantly smaller than experiment. The substitution of Ti for Fe in α-hematite was predicted to yield a net magnetic moment of $4\mu_B$ with polarization opposite to that of the Fe atom it replaced and one relatively delocalized carrier with moment parallel to that of the replaced Fe. Because the Ti atoms are known experimentally to prefer sites on the same sublattice, the results of those calculations implied that doping α-hematite with Ti produces a much larger carrier density in one spin channel than the other, an outcome which would have important implications for spintronics.

It has been pointed out, however, that the standard versions of density-functional theory (DFT) including LSDA-GGA may be deficient in describing systems in which strong electron-electron correlations are important.[8] This is particularly true for rare-earth metals for which DFT incorrectly predicts the f orbitals to be at the Fermi energy; for transition-metal impurities in alkaline metals, for which DFT predicts strong hybridization between the impurity and the host while in fact a localized magnetic moment is observed; as well as for transition-metal oxides for which DFT significantly underestimates band gaps and the size of local magnetic moments. Sometimes, it also incorrectly predicts a metallic ground state.[8]

Although much progress has been made in understanding the properties of transition-metal oxides, the understanding and especially the computation of their electronic structure are not nearly so straightforward as for materials such as metals and covalently bonded semiconductors. As we discuss below, band theory has serious difficulties in dealing with the strong electron-electron correlations in transition-metal ox-

ides. One approach to the electronic structure of these materials has been to build on the ideas of crystal-field theory.[9] A useful classification of transition-metal oxides has been made by Zaanen *et al.*[10] based upon the relative size of the *d*-*d* Coulomb interaction parameter U and the charge-transfer energy Δ which describes the energy associated with transfering a charge between a transition-metal atom and an oxygen. In their classification scheme, ''Mott-Hubbard'' insulators have a gap that separates cation *d* states, while ''charge-transfer'' insulators have a gap that separates anion *p* states (holes) and cation *d* states (electrons).

The simplest way to account for strong correlations within the context of density-functional theory is to add a Hubbard U term when electrons occupy the same site and orbital. This is the essence of the so-called LSDA+U approximation.[8,11,12] In this approach the electrons see an orbital dependent potential that depends on the occupation of the localized orbitals. In this paper, we use the LSDA+U approximation to study pure α-hematite and α-hematite doped with Ti and compare the results to standard density-functional theory. For consistency we use the local spin-density approximation to density-functional theory as a standard because the GGA version of DFT has not yet been generalized to consistently include the Hubbard U term.

Comparing LSDA and LSDA+U, we observe both quantitative and *qualitative* changes in the electronic structure. We observe, for example, that LSDA+U gives a significantly improved band gap for α-hematite and a larger magnetic moment. In both respects the agreement with experiment is significantly improved. In addition, the nature of the electronic states near the top of the valence band changes from Fe-*d* to O-*p* implying that, within the Zaanen *et al.* classification scheme, the nature of the insulating phase changes from ''Mott-Hubbard'' to charge transfer. Most importantly, use of LSDA+U for α-hematite(Ti) yields an entirely different picture of the electronic structure. Standard DFT techniques predict α-hematite(Ti) to be a magnetic half metal with relatively delocalized carriers, whereas LDA+U (with sufficiently large U) predicts that the doped material remains insulating with an impurity level localized on a single, particular Fe atom just below the Fermi energy.

Previous calculations on α-hematite include those using the local spin-density (LSDA) approach by Sandratskii *et al.*,[13] a Hartree-Fock based study by Catti *et al.*,[14] and an LSDA+U calculation by Punkkinen *et al.*[15] We will discuss the similarities and differences between our results and those of these authors in the text. We are not aware of previous calculations of the electronic and magnetic structure associated with Ti impurities in α-hematite.

There have also been a number of experimental studies aimed at elucidating the electronic structure of α-hematite. Photoemission studies which provide information about the occupied states of the electron spectrum have been reported by Fujimori *et al.*,[16] by Lad and Heinrich,[17] by Dräger *et al.*,[18] Bocquet *et al.*,[19] and by Kim *et al.*[20] Ultraviolet inverse photoemission spectroscopy[21] and x-ray absorption spectroscopy[22] have been used to probe the unoccupied part of the electron spectrum. The optical absorption edge was interpreted in terms of exciton and magnon effects by Galuza *et al.*[23] Benjelloun *et al.*[24] deduced a gap of $\approx$2.14 eV from optical data and $\approx$2.16 eV from transport measurements. This value is slightly less than the value of 2.36 eV that would be estimated from the transport data of Chang and Wagner.[25]

II. STRUCTURAL PROPERTIES

The electronic, structural, and magnetic properties of α-hematite and α-hematite(Ti) were calculated using both the LSDA and LSDA+U approximations. These were implemented within the VASP (Ref. 26) plane-wave code using projector augmented wave-based pseudopotentials. In the calculations, we used both 10 and 30 atom supercells for α-hematite, and 30 or 60 atom supercells for α-hematite(Ti). In the case of α-hematite(Ti) 50% (30 atom cell) or 25% (60 atom cell) of the Fe atoms in a particular layer were substituted by Ti. Nineteen k points in the irreducible Brillouin zone were typically used for the 10 atom cell calculations; five k points in the irreducible Brillouin zone were used for the 30 atom cell calculations; and one k point was used for the 60 atom cell calculations. We investigated the range of values for the Hubbard parameter from $U=0$ to $U=10$ eV.

Figure 1 shows the corundum structure of α-hematite. The structure can be viewed in various ways. One way consists of imagining a hexagonal close-packed lattice of oxygen atoms with two-thirds of the interstitial sites occupied by Fe atoms. Viewed in terms of the hexagonal cell, six formula units (30 atoms) are required. The oxygen atoms occur in layers along the z axis, three atoms per layer, within the hexagonal cell. Between each of these layers there are two Fe atoms in a noncoplanar arrangement.

The lattice can also be viewed as a rhombohedral cell with two formula units (10 atoms) per cell. In terms of this cell, the lattice is defined by the structural parameters[27] given in Table I. As reported in our previous paper, GGA does a relatively good job of reproducing this structure of α-hematite. Here, we find that LSDA also provides a relatively good description of its structural properties; however, we find in qualitative agreement with Punkkinen *et al.*[15] that LSDA+U reproduces the crystal structure even better. Comparison between the experimental and calculated parameters after relaxation is shown in Table I.

Each iron atom is surrounded by six oxygen atoms that form a distorted octahedron. Experimentally, three of the oxygen atoms are at 1.95 Å and other three are at 2.10 Å from the Fe. LSDA predicts these distances to be 1.92 Å and 2.13 Å. For LSDA+U ($U=5$ eV) the corresponding distances are 1.92 Å and 2.07 Å. Important structural quantities for determining the magnetic properties are the vectors connecting iron atoms through neighboring oxygen atoms. Neighboring Fe atoms within the same buckled plane are connected through oxygen atoms with bonds that make angles of 94°. For the adjacent buckled planes, the upper Fe atoms on the respective planes make an angle of 132° through the O between the planes. The angle between the lower atoms is also 132°. Lower Fe atoms on one plane make an angle of 87° with the upper Fe atoms on the plane

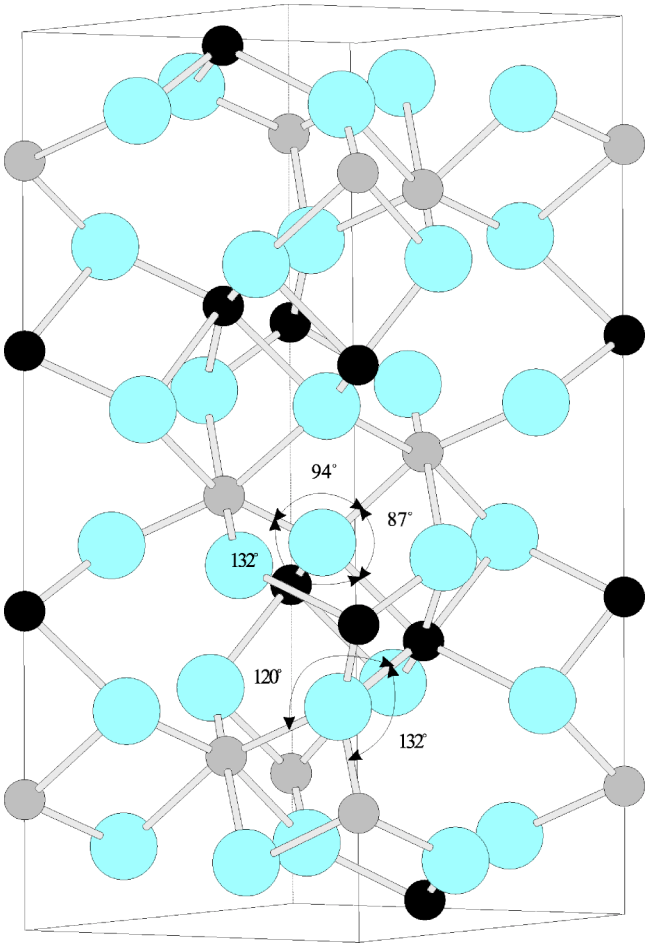

FIG. 1. Crystal structure of α-hematite. Large atoms are O. Smaller atoms are Fe. Different shading for the Fe atoms indicates atoms that are predominantly majority or minority spin.

above it and 120° with the upper Fe atoms on the plane below.

III. ELECTRONIC PROPERTIES

A. α-hematite

Figure 2 shows the electronic structure of α-hematite calculated using the LSDA for the 30 atom cell. The LSDA total density of states (DOS) for Fe_2O_3 is shown in Fig. 2(a), and the average DOS on the Fe and O sites is shown in Figs. 2(b) and 2(c), respectively. The compound is an antiferromagnetic insulator with a band gap of 0.31 eV. In Fig. 2(a) we also note the integrated density of states (IDOS) at certain energies for which the DOS is zero. These IDOS values together with the plots of the DOS on the individual atoms help us understand the origin and character of the states at different

TABLE I. Experimental, LSDA, and LSDA+U structural parameters for α-hematite. Parameters are given for the rhombohedral (10 atom) cell. U was taken to be 5 eV.

	Expt.	LSDA	LSDA+U
a(Å)	5.424	5.153	5.345
α	55°17′	53°50′	55°13′
u_1	0.355	0.347	0.354
x	0.552	0.560	0.556
y	−0.052	−0.064	−0.056
z	0.250	0.250	0.250

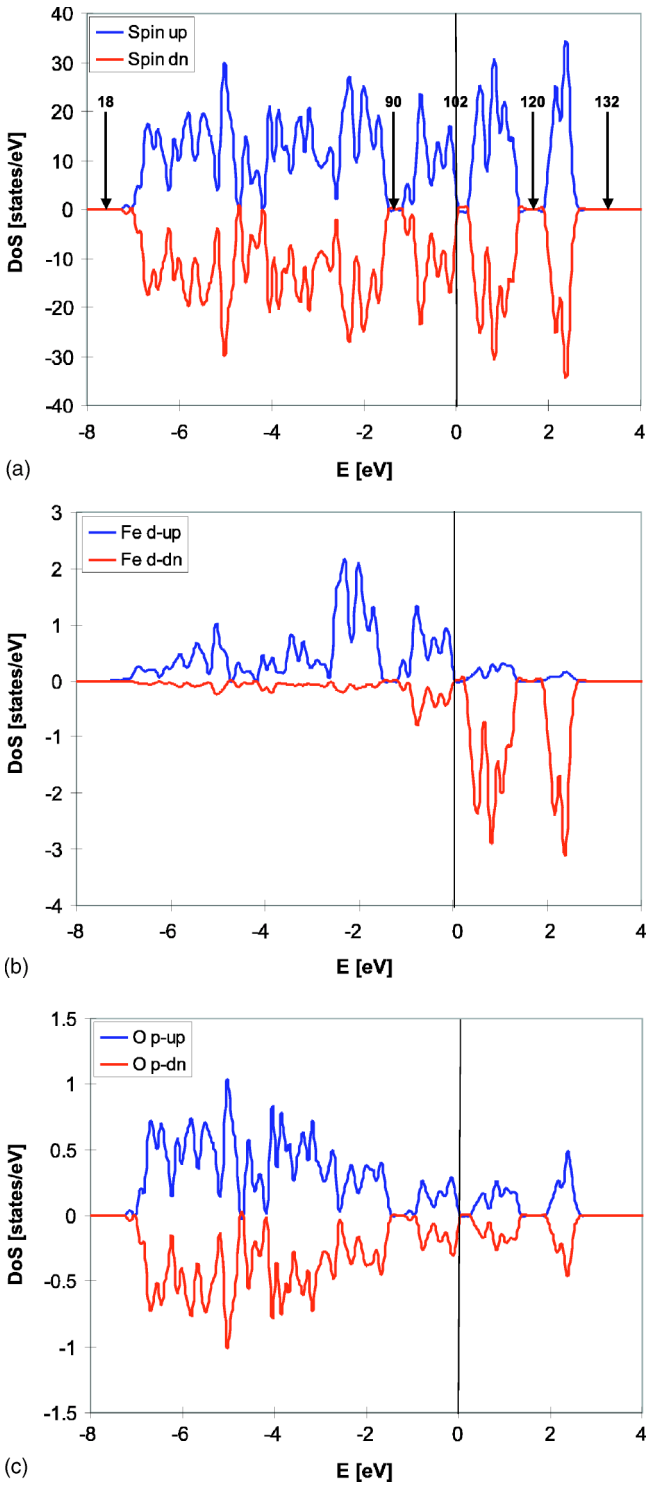

FIG. 2. LSDA density of states for α-hematite: (a) total DOS with integrated DOS, (b) d-DOS for Fe site within sphere of radius 0.45 Å, and (c) p-DOS for O site within radius of 1.46 Å.

energies. The lowest energy 18 spin states (not shown) are the 1*s* core states for the 18 oxygen atoms. The next 72 states (18–90) per spin channel are a combination of oxygen *p* states ($18\times3=54$) plus Fe-*d* states ($6\times3=18$). Because of the approximate octahedral symmetry, the *d* states split into three t_{2g}-like states and two e_g states. Because the octahedral symmetry is only approximate, the three t_{2g}-like states would further split into a singlet and doublet in a crystal-field analysis. This additional splitting is obscured by the band delocalization and hybridization. The 12 states (90–102) within ≈1 eV of the Fermi energy are primarily Fe-*d* e_g-like states with a small admixture of oxygen-*p*. The unoccupied states above the Fermi energy are divided into two groups, 18 t_{2g}-like states (102–120) and 12 e_g-like states.

Of the 12 Fe atoms in the 30 atom cell, six Fe atoms may be designated as ''up'' and six as ''down.'' We use up and down rather than ''majority'' and ''minority'' even though no spin axis is specified because the terms majority and minority are not appropriate for an antiferromagnet. Figure 2(b) shows the DOS for the Fe up sites. The DOS for the Fe down sites is its mirror image. From the analysis above we see that the Fe is in a high spin state with a nominal spin of 5/2. The calculated moment is $3.5\mu_B$ rather than $5\mu_B$, however, because the mean-field nature of the calculation allows some *d*-down spin density on the atoms that are primarily up-spin and vice versa. We shall see that this effect is greatly reduced by the inclusion of Coulomb correlations not included within LSDA.

The LSDA+*U* total DOS, the DOS on the Fe and O sites for Fe_2O_3 is shown in Figs. 3(a), 3(b), and 3(c), respectively. Just as for LSDA the lowest 18 states in both spin channels are the 1s states on the 18 oxygen atoms. The next 30 states in Fig. 3(a) are primarily the five occupied *d* states on each of the six up iron sites ($6\times5=30$). It can be seen that these bands are weakly hybridized with the oxygen *p* states. The next 54 states can be viewed as the oxygen *p* states, 3 per spin channel on each of the 18 oxygen atoms. It can be seen from Fig. 3(b) that these states have a relatively small admixture of Fe-*d* character. The next 18 states are almost purely unoccupied Fe-*d* t_{2g}-like states ($6\times3=18$) on the down sites. Finally there are 12 states that are purely Fe-*d* e_g-like states.

The two main differences between the LSDA electronic structure of α-hematite and the electronic structure with a nonzero *U* are the increased band gap and the decreased hybridization between the Fe-*d* and O-*p* states [Fig. 3(a)]. The band gap increases approximately proportional to *U* as the spin-up (occupied) bands and the spin-down (unoccupied) bands are now separated by *U*, which is the energy price for double occupancy. For $U=5$ eV, we obtain a band gap for α-hematite of 1.88 eV, slightly less than that has been deduced from experiment.[24]

In comparing our LSDA-DOS curves with previous work, we observe that our calculated electronic structure using LSDA agrees relatively well with that of Sandratskii and co-workers who used LSDA implemented within the atomic sphere approximation. This approximation required the introduction of empty spheres at strategic positions within the lattice to better fill the space in the relatively open corundum

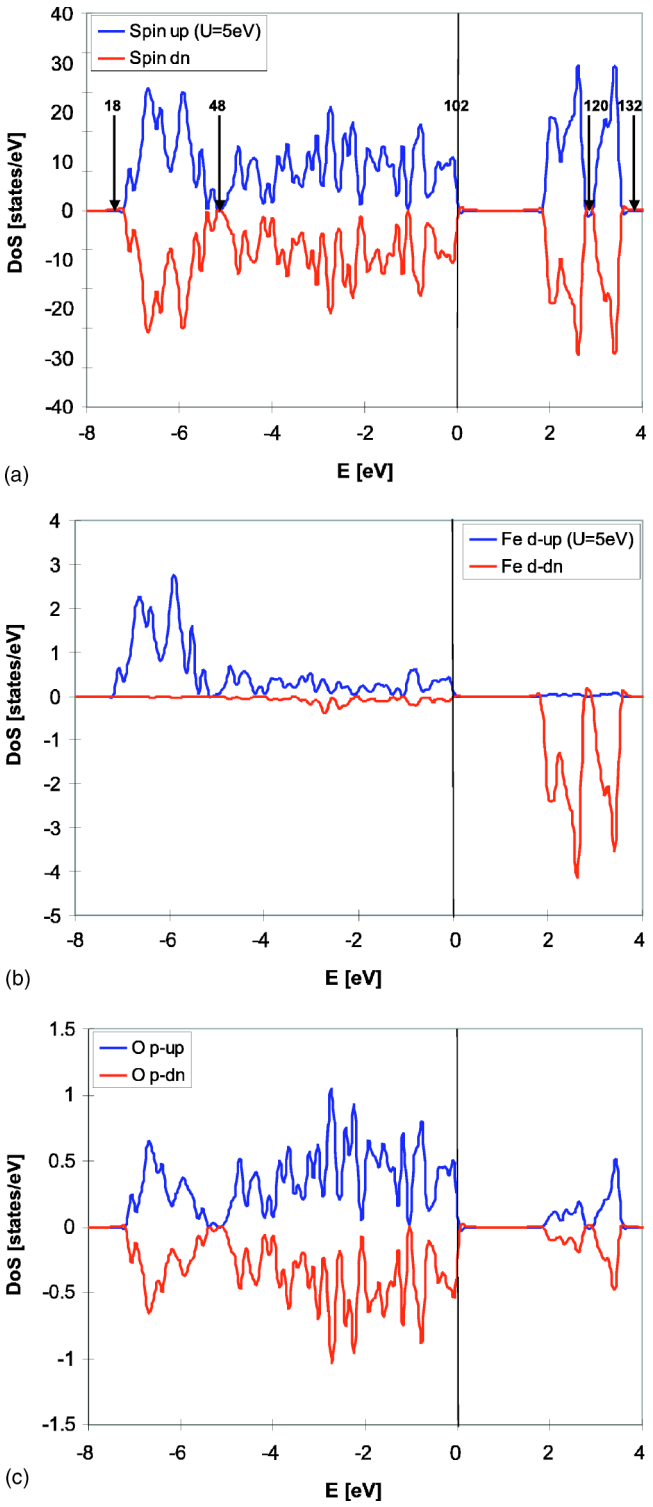

FIG. 3. LSDA+*U* density of states for α-hematite: (a) total with integrated, (b) Fe site, and (c) O site. In the case shown $U=5$ eV.

structure. Note that within the LSDA, the gap is primarily a gap between unfilled Fe-*d* e_g-like states and unfilled Fe-*d* t_{2g}-like states. Although there is some admixture of O-*p* states throughout both the filled and unfilled bands, the oxygen DOS is largely concentrated in a range of 1.5–7 eV below the top of the valence band. This means that LSDA-

hematite might be classified as a Mott-Hubbard insulator according to the scheme of Zaanen *et al.*[10]

Note that within LSDA, the occupied states on half of the Fe sites will be primarily up-spin with a small admixture of down, while the unoccupied states are primarily spin down with a small admixture of up. The primary effect of the Hubbard U parameter is to require an energy price proportional to U for this kind of double occupancy of spin states. This tends to make the d states on the Fe sites either pure up or pure down. It has the additional effect of separating the occupied d states from the unoccupied ones; and because Fe^{3+} nominally has five d electrons, it tends to separate the up bands from the unoccupied down-d bands and thereby increases the band gap.

Comparing our LSDA+U calculations with the Hartree-Fock calculations of Catti *et al.*,[14] we observe that qualitatively their results would be similar to that of a LSDA+U calculation with an extremely large U. Their calculated band gap of order 15 eV is much larger than the experimental value of ≈ 2 eV, and the very large separation between the filled d states and the oxygen p states seems to be contradicted by photoemission data. Indeed, the photoemission data were interpreted by Punkkinen *et al.* to imply a very small value of U, 2 eV. We believe that the Coulomb correlation effects are smaller than they would appear from the Hartree-Fock calculation, but larger than inferred by Punkkinen *et al.* We note that Fujimori *et al.*[16] utilized $U \approx 8$ eV (later reduced to 7 eV, Ref. 19) to fit their photoemission data. In addition, U of 2 eV leads to a very significant underestimate of the band gap and an underestimate of the magnetic moment on each site.

The difference between the LSDA and LSDA+U pictures arises from the increased energy cost of placing both an up-spin and a down-spin electron in the same Fe-derived d-orbital in LSDA+U. This causes the occupied Fe-d orbitals to be purely one spin direction. It also significantly reduces the hybridization between the occupied Fe-d states and the oxygen-p states. LSDA+U pushes the occupied d states below the oxygen-p states so that the band gap at the Fermi energy no longer separates occupied and unoccupied Fe-d states (Mott-Hubbard insulator), but occupied oxygen-p states and unoccupied Fe-d states (charge-transfer insulator). The energy penalty for double occupation of the d orbitals also increases the magnetic moment as is discussed in the following section.

B. α-hematite(Ti)

The effect of the Coulomb repulsion becomes more profound in the case of α-hematite doped with Ti. The LSDA calculation predicts a ferromagnetic metal with a moment of $4\mu_B$ per Ti [Fig. 4(a)] and a carrier in one of the spin channels. The picture in LSDA+U is qualitatively different. The system is predicted to remain insulating and a specific Fe atom becomes an Fe^{2+} ion.

When Ti is substituted for Fe, a Ti atom with four valence electrons replaces an Fe atom with eight valence electrons. Three of these four electrons are taken by the surrounding oxygen atoms leaving one electron for the Ti compared to

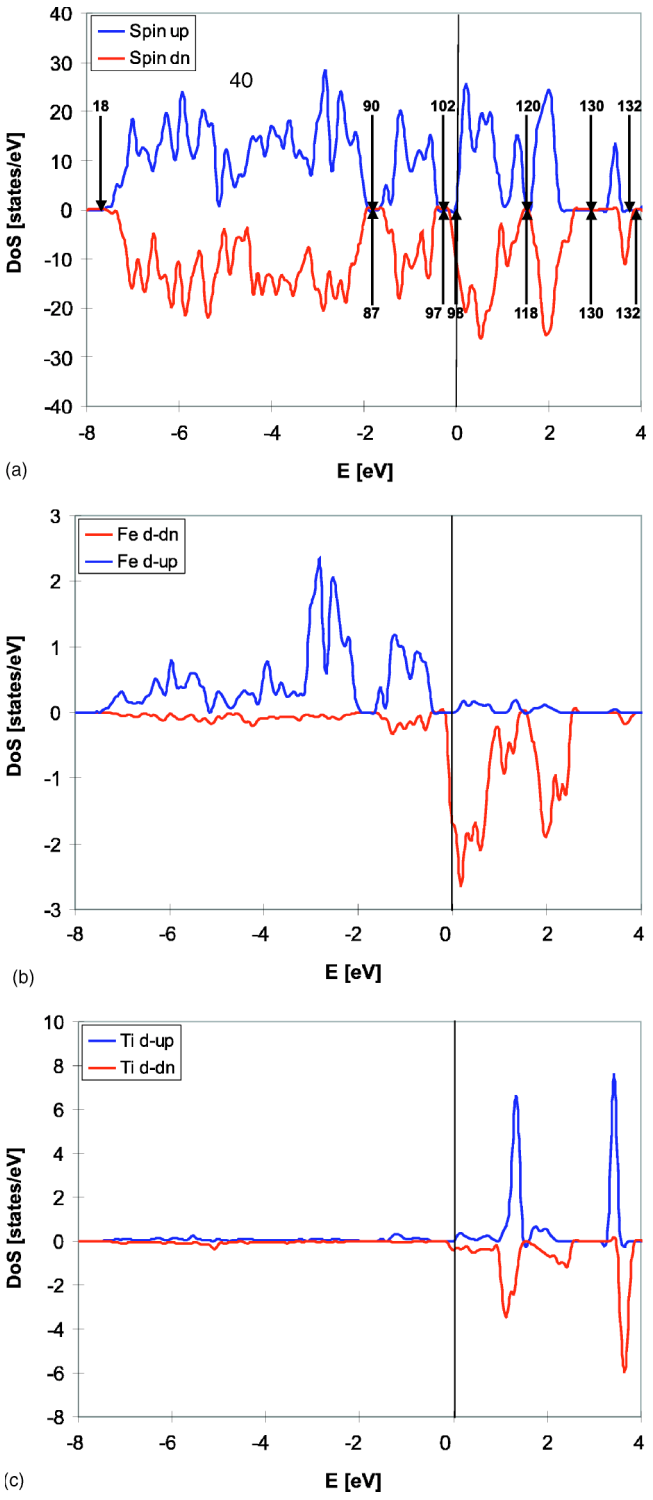

FIG. 4. LSDA density of states for α-hematite(Ti): (a) total with integrated, (b) generic Fe site, and (c) Ti site.

five electrons for the Fe. For both LSDA and LSDA+U the Ti d levels are higher than the Fe d levels as seen in Figs. 4(c) and 5(c) causing Ti to donate its remaining electron to the Fe atoms. Because the majority Fe states are filled, the donated electron must go into an Fe minority state. In principle, the electron could go into an unfilled minority d state on either an up layer or a down layer. We find that both in

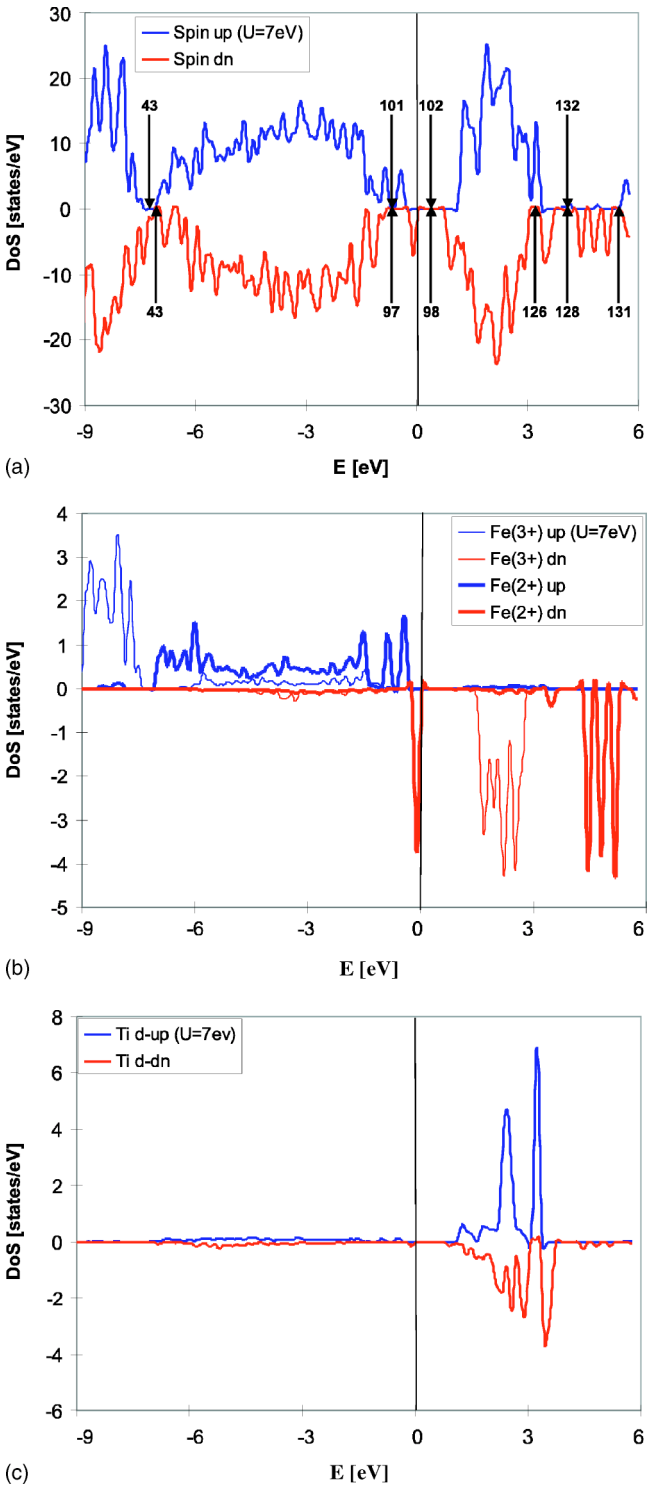

FIG. 5. LSDA+U density of states for α-hematite(Ti): (a) total with integrated, (b) an Fe^{3+} site (thin lines) compared to the Fe^{2+} site (thick lines), and (c) Ti site. In the case shown $U=7$ eV.

LSDA and in LSDA+U it chooses to go into an unfilled minority state on a layer with moments opposite to those in the layer for which the Ti substituted for the Fe. This means that the net moment resulting from the substitution is $4\mu_B$ $(5-1)$ rather than $6\mu_B$ $(5+1)$. The manner in which this electron is distributed, however, is completely different

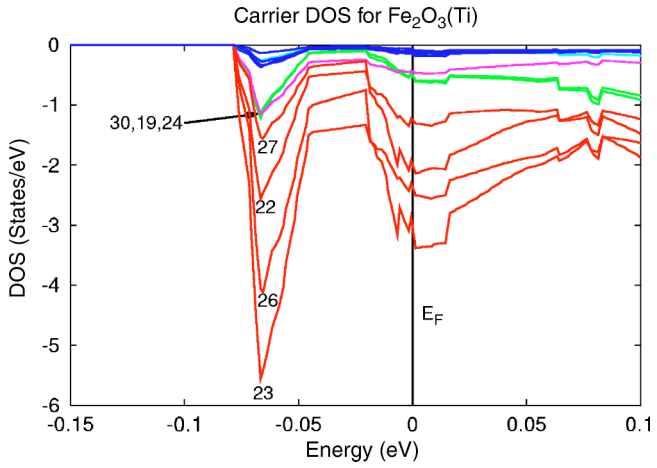

FIG. 6. This figure shows how the carrier is distributed among the Fe sites in LSDA. Sites 22 and 23 are in the Fe layer above the Ti impurity, and sites 26 and 27 are in the Fe layer below the impurity. Sites 19 and 30 are three Fe layers above or below the impurity. Site 24 is the Ti impurity site.

in the two cases. For LSDA, the electron is distributed over all of the Fe atoms with moment direction opposite to that of the substituted Fe as shown in Fig. 6. Thus the LSDA (or GGA) predict a relatively delocalized carrier. For LDA $+U$, however, the extra electron is localized both spatially and energetically. A very narrow peak appears separated from the top of the valence band that holds one electron which is localized on a particular Fe atom on one of the Fe layers adjacent to the Ti. Thus, within LDA+U, the system acts as if substitution of Ti causes the formation of an Fe^{2+} state on a particular Fe atom. This atom is not the closest to the Ti, but would be the closest if distances were measured indirectly through a connecting oxygen atom.

The process just described is a fairly general illustration of the effect of U on the impurity states in transition-metal oxides. Depending on the position of the impurity levels with respect to the unoccupied levels of the host material, the impurity electron(s) can either stay on the impurity site forming a local moment or they can be donated to the host atoms. If the band is not degenerate, this will immediately produce an insulator. If the band is degenerate the material will remain a metal unless a distortion of the lattice reduces the symmetry sufficiently to remove the degeneracy. In our case, the trigonal symmetry about the Fe site removes the degeneracy.

IV. MAGNETIC PROPERTIES

Magnetically, α-hematite is antiferromagnetic with the Fe atoms in the buckled planes perpendicular to the c axis being coupled ferromagnetically with antiferromagnetic interactions between the planes. This same structure is obtained in our calculations, the difference in energy between the ferromagnetic and antiferromagnetic ground states being ≈ 0.7 eV per formula unit for both LSDA and LSDA+U. This value is somewhat less than the value of 1.0 eV calculated by Sandratskii *et al.*[13] and should be more consistent with the experimental Néel temperature of 953 K based on

TABLE II. Band gap (ΔE) and magnetic moment per Fe (M) as a function of U for α-hematite. The exchange parameter J is fixed to 0.9 eV.

U (eV)	1.0	2.0	3.0	4.0	5.0	7.0	10.0
ΔE (eV)	0.35	0.78	1.09	1.45	1.88	2.57	3.61
$M(\mu_B)$	3.37	3.70	3.88	4.01	4.11	4.26	4.46

their scheme for estimating the T_C. The Hartree-Fock calculation[14] predicts a value less than 0.1 eV per formula unit which seems unphysically low.

The ferromagnetic interactions within the planes can be rationalized in terms of the fact that the Fe-O-Fe angles within the plane are close to 90°, a condition which is often associated with ferromagnetic interactions in transition-metal oxides. The antiferromagnetic interactions between the planes might also be expected from the Fe-O-Fe angles which are larger (132° or 120°).

We obtained the average magnetic moment on the Fe sites by integrating the absolute value of the magnetization density over the 30 atom cell and dividing by 12, the number of Fe atoms. This procedure yields a magnetic moment of $3.5\mu_B$ per Fe in LSDA. This is less than the $5\mu_B$ that might have been expected in a simple model in which the Fe atoms are assumed to be Fe^{3+}. This would leave five electrons on the Fe atoms and if Hund's first rule were applied one might expect a moment of $5\mu_B$. The experimental moment has been reported to be $4.6–4.9\mu_B$.[28] Our calculated moment for LSDA is in reasonable agreement with that calculated by Sandratskii *et al.*[13] who calculated a moment of $3.72\mu_B$ per Fe atom in a calculation which used LSDA and an atomic sphere approximation.

Including Coulomb correlations reduces the number of occupied down-spin electron states on the Fe sites that are predominantly up-spin because the double occupancy of a d orbital now incurs an energy penalty. Thus our LSDA+U calculation with $U=5$ eV yields a magnetic moment per Fe of $4.1\mu_B$. The calculated moment per Fe atom as a function of U is given in Table II. These moment values were calculated similar to the calculations for LSDA by integrating the absolute value of the magnetization density over the cell. For comparison, Punkkinen *et al.*[15] obtained a moment of $3.4\mu_B$ per Fe atom using LDA+U with $U=2$ eV and Catti *et al.*[14] estimated a moment of $4.7\mu_B$ using a Mulliken analysis.

We also were able to converge α-hematite in a ferromagnetic phase using both LSDA and LSDA+U with $U=5$ eV. LSDA yields a magnetic moment of $2.67\mu_B$ per Fe atom, while LSDA+U with $U=5$ eV yields a moment of $5.000\mu_B$/Fe.

V. VARIATION WITH U

We also study the effects of different values of U on the band gap and moment per Fe site in α-hematite. The band gap is grossly underestimated by the LSDA approximation. In Table II, the dependence of the band gap and the size of the magnetic moment on U is illustrated. The correct value for the band gap of α-hematite is obtained for $U=5$ eV. The magnetic moment is calculated as the total magnetic moment magnitude divided by the number of Fe atoms in the supercell. For $U\approx 5$-6 eV the magnetic moment is obtained to be $4.11\mu_B$ per Fe at $U=5$ eV. The above results show that LSDA+U, with $U\approx 5$ eV, corrects the most obvious shortcomings of LSDA. The band-gap size increases by more than six times to 1.88 eV which compares reasonably well to the experimental value of 2.1 eV.[24] The magnetic moment increases by $0.6\mu_B$ which brings it much closer to the experimental estimates of $(4.6–4.9)\mu_B$.[28]

In the case of α-hematite(Ti), for low values of U (up to 2 eV) the system remains a metal as in the LSDA prediction. However, the DOS reveals a state forming out of the conduction band. At $U=5$ eV, a localized state just below the Fermi surface has formed but the band gap is very small. At $U>6$ eV, the localized state is well separated from the upper (unoccupied) bands. This metal-insulator transition occurs between $U=2$ and 3 eV.

VI. CONCLUSIONS

Mean-field electronic structure theory (LDA) appears to provide a good description of the structural and magnetic properties of α-hematite. The inclusion of correlations in the mean-field theory (LSDA+U) improves the structural parameters and the size of the magnetic moment. However, the main impact of the electron-electron correlations is observed in the calculated electronic structure of α-hematite and α-hematite(Ti). Both methods predict α-hematite to be an insulator, but LSDA+U gives the correct band gap and a larger magnetic moment. The substitution of Ti for Fe in α-hematite is predicted to yield a net magnetic moment of $4\mu_B$ of polarization opposite to that of the Fe atom it replaced. However, LSDA gives a mean-field-like picture in which the additional electron donated by the Ti^{4+} impurity is delocalized over the Fe atoms with the moment opposite to that of the substituted Fe atom. This behavior gives rise to itinerant d electrons and metallic band structure. On the other hand, LSDA+U predicts that the extra d electron is localized on a particular Fe atom, thus providing a chemistrylike picture in which each Ti that substitutes for an Fe^{3+} cation produces an Fe^{2+} cation located at a particular position relative to the Ti impurity.

ACKNOWLEDGMENTS

This research was supported by Office of Basic Energy Science of the U.S. Department of Energy and by the National Science Foundation, Grant No. DMR0213985. Part of this research was supported by the Oak Ridge Institute for Science and Education and the Oak Ridge National Laboratory. ORNL is operated by UT-Batelle, LLC for U.S. DOE under Contract No. DE-AC05-000R2275. We thank Professor Vladimir Anisimov for helpful comments.

[1] H. Munekata, H. Ohno, S. von Molnar, A. Segmuller, L.L. Chang, and L. Esaki, Phys. Rev. Lett. **63**, 1849 (1989).
[2] H. Ohno, Physica E (Amsterdam) **6**, 702 (2000); H. Ohno and F. Matsukura, Solid State Commun. **117**, 179 (2001).
[3] S. Sonoda, S. Shimizu, T. Sasaki, Y. Yamanoto, and H. Hori, J. Cryst. Growth **237**, 1358 (2002); G.T. Thaler, M.E. Overberg, B. Gila, R. Frazier, C.R. Abernathy, S.J. Pearton, J.S. Lee, S.Y. Lee, Y.D. Park, Z.G. Khim, J. Kim, and F. Ren, Appl. Phys. Lett. **80**, 3964 (2002).
[4] N. Theodoropoulou, A.F. Hebard, S.N.G. Chu, M.E. Overberg, C.R. Abernathy, S.J. Pearton, R.G. Wilson, and J.M. Zavada, J. Appl. Phys. **91**, 7499 (2002).
[5] Y. Ishikawa and S. Akimoto, J. Phys. Soc. Jpn. **12**, 1083 (1957).
[6] Y. Ishikawa, J. Phys. Soc. Jpn. **13**, 37 (1958).
[7] W.H. Butler, A. Bandyopadhyay, and R. Srinivasan, J. Appl. Phys. **93**, 7882 (2003).
[8] V.I. Anisimov, F. Aryasetiawan, and A.I. Lichtenstein, J. Phys.: Condens. Matter **9**, 767 (1997).
[9] G. F. Dionne, in *Magnetic Interactions and Spin Transport*, edited by A. Chtchelkanova, S.A. Wolf, and Y. Idzerda (Kluwer Academic, New York, 2003).
[10] J. Zaanen, G.A. Sawatzky, and J.W. Allen, Phys. Rev. Lett. **55**, 418 (1985).
[11] I.V. Solovyev, P.H. Dederichs, and V.I. Anisimov, Phys. Rev. B **50**, 16 861 (1994).
[12] V.V. Nemoshkalenko and V.N. Antonov, *Computational Methods in Solid State Physics* (Taylor and Francis, London, 1999).
[13] L.M. Sandratskii, M. Uhl, and J. Kübler, J. Phys.: Condens. Matter **8**, 983 (1996); L.M. Sandratskii and J. Kübler, Europhys. Lett. **33**, 447 (1996).
[14] M. Catti, G. Valerio, and R. Dovesi, Phys. Rev. B **51**, 7441 (1995).
[15] M.P.J. Punkkinen, K. Kokko, W. Hergert, and I.J. Väyrybeb, J. Phys.: Condens. Matter **11**, 2341 (1999).
[16] A. Fujimori, M. Saeki, N. Kimizuka, M. Taniguchi, and S. Suga, Phys. Rev. B **34**, 7318 (1986).
[17] R.J. Lad and V.E. Henrich, Phys. Rev. B **39**, 13 478 (1989).
[18] G. Dräger, W. Czolbe, and J.A. Leiro, Phys. Rev. **45**, 8283 (1992).
[19] A.E. Bocquet, T. Mizokawa, T. Saitoh, H. Namatame, and A. Fujimori, Phys. Rev. B **46**, 3771 (1992).
[20] C.-Y. Kim, M.J. Bedzyk, E.J. Nelson, J.C. Woicik, and L.E. Berman, Phys. Rev. B **66**, 085115 (2002).
[21] F. Ciccacci, L. Braicovich, E. Puppin, and E. Vescovo, Phys. Rev. B **44**, 10 444 (1991).
[22] F.M.F. deGroot, M. Grioni, J.C. Fuggle, J. Ghijsen, G.A. Sawatzky, and H. Petersen, Phys. Rev. B **40**, 5715 (1989).
[23] A.I. Galuza, A.B. Beznosov, and V.V. Eremenko, Low Temp. Phys. **24**, 726 (1998).
[24] D. Benjelloun, J.-P. Bonnet, J.-P. Doumerc, J.-C. Launay, M. Onillon, and Paul Hagenmuller, Mater. Chem. Phys. **10**, 503 (1984).
[25] R.H. Chang and J.B. Wagner, J. Am. Ceram. Soc. **55**, 211 (1972).
[26] G. Kresse and J. Hafner, Phys. Rev. B **47**, 558 (1993); **49**, 14 251 (1994); G. Kresse and J. Furthmüller, Comput. Mater. Sci. **6**, 15 (1996); G. Kresse and J. Furthmüller, Phys. Rev. B **54**, 11 169 (1996).
[27] G. Shirane, D.E. Cox, W.J. Takei, and S.L. Ruby, J. Phys. Soc. Jpn. **17**, 1598 (1962).
[28] J.M.D. Coey and G.A. Sawatsky, J. Phys. C **4**, 2386 (1971); E. Kren, P. Szabo, and G. Konczos, Phys. Lett. **19**, 103 (1965).